

Optical spectroscopy of plasmons and excitons in cuprate superconductors

D. van der Marel

¹*Département de Physique de la Matière Condensée,
Université de Genève, CH-1211 Genève 4, Switzerland*

(Dated: February 2, 2008)

An introduction is given to collective modes in layered, high T_c superconductors. An experimental demonstration is treated of the mechanism proposed by Anderson whereby photons travelling inside the superconductor become massive, when the U(1) gauge symmetry is broken in the superconductor to which the photons are coupled. Using the Ferrell-Tinkham sumrule the photon mass is shown to have a simple relation to the spectral weight of the condensate. Various forms of Josephson plasmons can exist in single-layer, and bi-layer cuprates. In the bi-layer cuprates a transverse optical plasma mode can be observed as a peak in the c -axis optical conductivity. This mode appears as a consequence of the existence of two different intrinsic Josephson couplings between the CuO_2 layers. It is strongly related to a collective oscillation corresponding to small fluctuations of the relative phases of the two condensates, which has been predicted in 1966 by A.J. Leggett for superconductors with two bands of charge carriers. A description is given of optical data of the high T_c cuprates demonstrating the presence of these and similar collective modes.

I. INTRODUCTION

Electrons form, together with the atomic nuclei, the basic fabric of materials. In order to expose the organizing principles of matter, experimental physicists take apart the complicated fabric of matter, aimed with a vast array of different spectroscopic methods. Spectroscopic tools typically expose the sample to an external field or a beam of particles, and one measures the response of the sample to this external stimulus. Most of the spectroscopic tools, such as optical absorption or inelastic scattering, do not reveal the nuclei or the electrons directly. Instead one observes a spectrum of excited states which typically involve the excitation of several or many electrons and/or nuclei simultaneously.

The reason is, of course, that the elementary particles forming a solid behave in a correlated way, and this is already the case for the ground state of the material. As a result one can not excite a single electron without influencing the state of the other particles in its vicinity. Usually, if the amplitudes are not too large, the excitations can be treated in the harmonic approximation. Regardless of the details of the material and of the type of interactions between the particles one can, in principle and at least for small amplitudes, identify a set of fundamental modes in the harmonic approximation. These so-called collective modes form an orthogonal set of eigenstates of the material. To treat the electrical transport properties of metals it is usually much simpler to refer to the language of electrons and holes. Nevertheless, even for simple metals like aluminum or sodium, the metallic luster is caused by the plasma oscillations, which are one out of several possible collective modes in a conducting material.

One of the relevant features of collective excitations is, that they provide the dynamical fluctuations transforming between different states of matter. They can be populated either by varying the temperature or by applying and external field, for example an electrical field,

pressure, or magnetism. Broken symmetries are typically accompanied by collective modes. We will now discuss a few examples:

(1) The phase of the order parameter in a superconductor is an example of a spontaneously broken U(1) symmetry. This implies that the ground state is not unique but has a continuous degeneracy. In neutral superfluid the fluctuations of this phase then possess linear dispersion^{1,2,3}.

(2) Earlier Anderson had shown from the gauge-invariant treatment required for the Meissner effect, and taking into account the long range nature of the Coulomb interactions, that in a superconductor the longitudinal modes are massive^{4,5,6}, and that the transverse electromagnetic waves travelling in a superconductor acquire a mass due to their coupling to the superconducting condensate. An experimental example of this effect is shown in Fig. 1. A detailed discussion of these data follows in section VI.

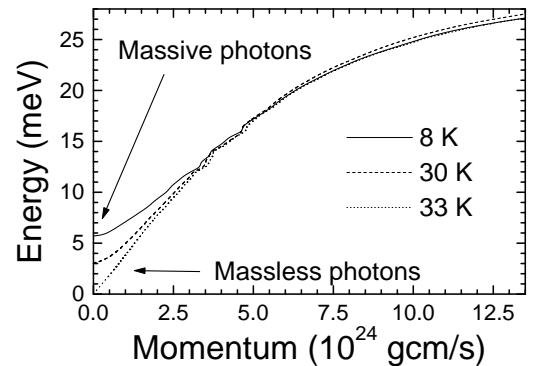


FIG. 1: Energy-momentum dispersion of photons polarized along the c -direction in $\text{La}_{1.85}\text{Sr}_{0.15}\text{CuO}_{4+\delta}$ for different temperatures. T_c of this sample is 33 K. The photons travelling inside the superconductor become massive, when the U(1) gauge symmetry is broken in the superconductor to which the photons are coupled.

Superconductivity	Electroweak symmetry breaking
Spontaneous symmetry breaking of the pairing order parameter, ψ .	Spontaneous symmetry breaking of the Higgs field, Φ .
Amplitudon	Higgs particle
The Goldstone mode of the phase of the order parameter has a gapless sound-dispersion	
The electromagnetic field, A_μ , has a gapless sound-like dispersion.	The $W^{+/-}$ and Z gauge fields have a gapless sound-like dispersion.
Coupling between the order-parameter and the EM-field: $(\partial_\mu + iqA_\mu)\psi$	Coupling between the Higgs-field and the $W^{+/-}, Z$ fields: $(2\partial_\mu + ig\tau \cdot W_\mu + ig' B_\mu Y)\Phi$
The coupling makes the gauge particles massive	
Massive photons	Massive $W^{+/-}, Z$ particles

TABLE I: Some analogies between the theory of superconductivity and the electro-weak theory.

(3) Anderson's mechanism was later used in the context of elementary particle physics to predict, among other things, the occurrence of a novel massive elementary particle due to spontaneous symmetry breaking, the Higgs boson, and to show that the W and Z bosons acquire a finite mass due to the coupling to the symmetry broken Higgs-field^{4,5,7,8,9}. The analogy between the theory of superconductivity and the electro-weak theory is summarized in table I.

(4) The collective modes spectrum of the amplitude of the order parameter of a superconductor has a gap, which has been observed experimentally in NbSe₂ with Raman spectroscopy, and which plays role equivalent to

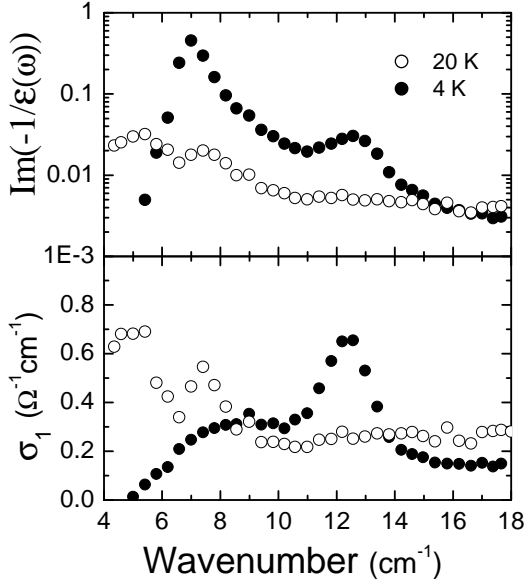


FIG. 2: The c -axis optical conductivity and loss-function, of SmLa_{0.8}Sr_{0.2}CuO_{4- δ} for 4 K (closed symbols), and 20 K (open symbols). T_c of this sample is 16 K. When the sample enters the superconducting state, two longitudinal collective modes appear (7 and 12.8 cm⁻¹) and one with transverse polarization (12.1 cm⁻¹). The two modes near 12 cm⁻¹ correspond to relative phase fluctuations of the two copper-oxygen layers within the unit cell¹⁰.

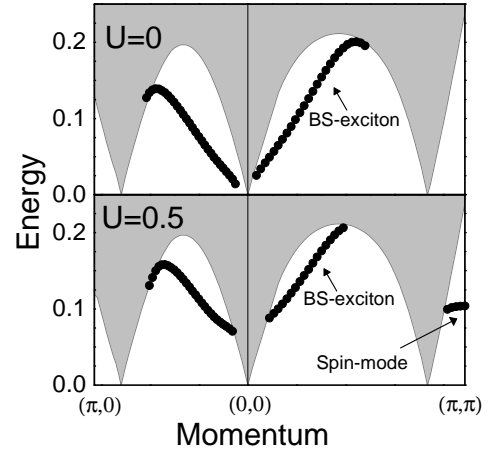


FIG. 3: RPA calculation of the collective modes of a layered d-wave superconductor using a tight-binding calculation, reproduced from Ref.11. Below the particle-hole continuum two types of modes occur: A fluctuation between d-wave and s-wave pairing symmetry of the variety predicted by Bardasis and Schrieffer¹² and a spin-fluctuation near the (π, π) point. The plasma-mode along the planes is at a much higher energy, not visible in this diagram.

the Higgs particle in the electro-weak theory^{13,15?}.

(5) An unusual type of exciton has been predicted by Leggett for the case where a superconducting gap occurs in two or more overlapping bands¹⁶ provided that a weak Josephson-coupling between those bands is present. A similar type of exciton is expected for the case where the crystal structure contains pairs of weakly coupled two-dimensional layers^{17,18}. For the latter case the Coulomb interaction between the layers plays a dominant role. An experimental example is shown in Fig. 2. A detailed discussion of these data follows in section XIII.

(6) Motivated by the observation of a precursor infrared absorption in Pb and Hg by Ginsberg, Richards, and Tinkham¹⁹, Bardasis and Schrieffer have predicted excitons in the superconducting gap, corresponding to pairing symmetries different from those of the ground state^{12,20}. Fig. 3 shows an example of such a mode in a model where the pairing-interaction has both an s-wave and a d-wave channel. In the absence of a local repulsive potential, the calculation predicts a soft excitonic mode near $k = (0,0)$, which corresponds to a transition from s-wave to d-wave order parameter. Increasing the on-site interaction results in an increase of the energy of this exciton, implying that the d-wave order parameter becomes more stable compared to s-wave symmetry.

(7) A paramagnetic Fermi-liquid is composed of two degenerate liquids of opposite spin. The plasma-oscillations discussed above correspond to an in-phase modulation of the two spin-densities. The out-of-phase modulation is called a paramagnon. Because the two spin-liquids oscillate out of phase, there is no net charge-displacement, and consequently there is no restoring electric force in contrast to the in-phase plasma oscillations.

These modes are therefore inside the particle-hole continuum and they are normally overdamped. However, if the particle-hole continuum is gapped, as happens in the superconducting state, a paramagnon branch can occur below the particle-hole continuum, with a correspondingly weak damping. In order to exist on an energy scale below the superconducting gap, the paramagnon must be very soft, implying that the system has been tuned close to a spin-density wave instability. In Fig. 3 an example of this fine-tuning is given, which was calculated using the generalized random phase approximation scheme by Anderson⁴, Bogoliubov, Tolmachev and Shirlov¹. Increasing a local repulsive interaction vertex U from zero to 0.5, results in the emergence of a soft spin-density mode near the (π, π) point. Similar behaviour has been observed with inelastic neutron scattering in the cuprate superconductors^{21,22}, where indeed a transition takes place to a spin ordered state when the Mott-insulating state is approached by tuning the carrier concentration.

(8) Various additional collective modes have been identified, which are associated with a rotation between different order parameters permitted by models containing additional symmetries. Examples are the SO(4) symmetry of the negative U Hubbard model²³, the SO(5) symmetry²⁴ and the SU(2) symmetry groups²⁵, where the latter two have been proposed in the context of the t-J model. The complex order parameter permitted by these models corresponds to a rich and complicated spectrum of collective modes. The SO(5) model generates a bosonic excitation with spin quantum number $S = 1$ and momentum (π, π) . This mode has been proposed for the resonance with the same quantum numbers in the cuprates, which has been observed with inelastic neutron scattering²⁶.

The superfluid phases of He³ provide particularly beautiful examples where several of the collective modes mentioned above (and several others which are not in this list) have been observed experimentally²⁷. In this article we will concentrate mostly on collective modes which can be observed with optical spectroscopy, i.e. items 1 to 6 of the previous list involving flow of charge and current. Because the cuprates are strongly correlated materials, and many of their properties can not be explained within the context of the random phase approximation, a large part of the subsequent discussion will be based on classical field theory. The penalty one pays for this, is that the properties which one can address with such a formalism are limited to a particular set of collective modes. The advantage is, that the results calculated with such a model do not heavily rely on details on the microscopic level.

II. SOUND AND PLASMONS

We begin by discussing the collective mode spectrum of a classical compressible fluid of interacting particles

of charge e^* in a charge-compensating background. The compressibility of the fluid is $\kappa = n^{-2} \partial n / \partial \mu$, which is a scalar. The mass of the particles, m , is in some cases an anisotropic tensor. The fluctuations of the particle density around its equilibrium value are described by the field $n(r, t) = n^{tot}(r, t) - n_0$. We furthermore allow the coupling of the fluid to an electromagnetic field, $\vec{E}(r, t) = -\vec{\nabla} \phi(r, t) - c^{-1} d\vec{A}(r, t)/dt$, $\vec{B}(r, t) = \vec{\nabla} \times \vec{A}(r, t)$. The dynamical behaviour of such a fluid can be described with the Hamiltonian²⁸

$$H = \int \left(\vec{\pi} - \frac{e^* \vec{A}}{c} \right) \cdot \frac{n_0}{2\bar{m}} \cdot \left(\vec{\pi} - \frac{e^* \vec{A}}{c} \right) d^3r + \int \frac{|n(r)|^2}{2\kappa n_0^2} d^3r \\ + \int \int \frac{e^{*2} n(r) n(r')}{2|r-r'|} d^3r d^3r' + \int e^* \phi(r) n(r) d^3r \quad (1)$$

where

$$\vec{\pi} \equiv \vec{\nabla} \nu(r) + \vec{\nabla} \times \vec{\mu}(r)$$

The first set of Hamiltonian equations of motion for the longitudinal currents are $dn/dt = \delta \mathcal{H} / \delta \nu = \partial \mathcal{H} / \partial \nu - \vec{\nabla} \cdot \partial \mathcal{H} / \partial (\vec{\nabla} \nu)$, and $-d\nu/dt = \delta \mathcal{H} / \delta n$. The second set for the transverse currents is $d\vec{\eta}/dt = \delta \mathcal{H} / \delta \vec{\mu} = \partial \mathcal{H} / \partial \vec{\mu} + \vec{\nabla} \times \partial \mathcal{H} / \partial (\vec{\nabla} \times \vec{\mu})$, and $-d\vec{\mu}/dt = \delta \mathcal{H} / \delta \vec{\eta}$. The potential energy does not depend on $\vec{\eta}$, because a liquid has zero shear-modulus. This provides four coupled relations between the currents and the density fluctuations

$$-\frac{d}{dt} \nu(r) = \frac{n(r)}{\kappa n_0^2} + e^{*2} \int d^3r' \frac{n(r')}{|r-r'|} + e^* \phi(r) + \frac{\nu(r)}{\tau} \\ -\frac{d}{dt} \vec{\mu}(r) = 0 \quad (2) \\ \frac{d}{dt} n(r) = -\vec{\nabla} \cdot \frac{n_0}{\bar{m}} \cdot \left(\vec{\nabla} \nu(r) + \vec{\nabla} \times \vec{\mu}(r) - \frac{e^* \vec{A}(r)}{c} \right) \\ \frac{d}{dt} \vec{\eta}(r) = \vec{\nabla} \times \frac{n_0}{\bar{m}} \cdot \left(\vec{\nabla} \nu(r) + \vec{\nabla} \times \vec{\mu}(r) - \frac{e^* \vec{A}(r)}{c} \right)$$

where the last term of the first line was introduced to represent the effect of dissipation on the current. Combining these expressions we obtain the wave-equation

$$n_0 e^* \vec{\nabla} \cdot \frac{1}{\bar{m}} \cdot \vec{E}(r) + \left\{ \frac{d^2}{dt^2} + \frac{1}{\tau} \frac{d}{dt} \right\} n(r) \\ = \vec{\nabla} \cdot \frac{1}{\bar{m}} \cdot \vec{\nabla} \left\{ \frac{n(r)}{\kappa n_0} + e^{*2} n_0 \int d^3r' \frac{n(r')}{|r-r'|} \right\} \quad (3)$$

for the propagation of density fluctuations, or plasmons, of a charged fluid²⁹. For plane waves $\vec{E}(r, t) = \vec{E}_k e^{ik \cdot r - i\omega t}$, $n(r, t) = n_k e^{ik \cdot r - i\omega t}$, this amounts to

$$\left(\omega^2 + \frac{i\omega}{\tau} - \vec{k} \cdot \left[\frac{\omega_p^2}{|\vec{k}|^2} + \vec{v}_s^2 \right] \cdot \vec{k} \right) n_k = i\vec{k} \cdot \frac{e^* n_0}{\bar{m}} \cdot \vec{E}_k \quad (4)$$

where $\omega_p = (4\pi n_0 e^{*2} / m)^{1/2}$ is the plasma frequency and $v_s = (\kappa n_0 m)^{-1/2}$ is the sound-velocity. We should keep in mind that m , ω_p^2 and v_s^2 are tensors: when the mass-tensor is anisotropic, the plasma-frequency and its dispersion depend on the direction of propagation in the medium.

III. ISOTROPIC PLASMON-DISPERSION

Let us first consider the case of an isotropic charged fluid. In this case the plane wave solutions obey the dispersion relation

$$\omega(k)^2 = \omega_p^2 + v_s^2 k^2 \quad (5)$$

In a 3D Fermi gas the compressibility arises purely from the density of states at the Fermi energy: $\kappa = n^{-2} dn/d\mu = 3/(mv_F^2 n)$, and consequently the zero-sound velocity is³⁰ $v_s = 3^{-1/2} v_F$. If we apply Eq. 5 to this case, we obtain $\omega_k = \omega_p + \frac{v_F^2}{6\omega_p} k^2 + O(k^4)$ for the dispersion formula. Although this resembles the result obtained with the random phase approximation (RPA) of the electron gas model³⁰ $\omega^{RPA} = \omega_p + \frac{3v_F^2}{10\omega_p} k^2 + O(k^4)$ the dispersive term in the RPA is a factor $9/5$ larger, which shrinks to a value closer to 1 when higher order electron-correlation diagrams are included in the calculation^{30,31}. In the alkali metals a systematic reduction has been observed with high energy electron energy loss spectroscopy as the relative importance of the Coulomb interaction increases³². It is important to point out here, that at a qualitative level the dispersion of the plasma modes does not rely on the fact that microscopically the particles in the fluid are fermions. Indeed, Eq. 5 expresses a rather generic feature of a liquid, namely that it has a finite compressibility. For this reason Eq. 5 has a broad applicability, which goes beyond the special case of a Fermi-gas. This becomes particularly important in cases where on a microscopic level the properties are not fully understood, like in the cuprate materials: In spite of the lack of a fully established microscopic framework it is still possible to predict a certain number of properties at least at a qualitative level, in particular the collective plasma modes.

Superconductors are characterized by a macroscopic coherent state $\psi(r, t)$. Usually it is assumed that the variations of the amplitude are negligibly small, hence $\psi(r, t) = n_0^{1/2} \exp\{i\varphi(r, t)\}$. In this case the macroscopic current and the density of such a state are

$$n(r, t) = |\psi(r, t)|^2 = n_0 \quad (6a)$$

$$\vec{j}(r, t) = -\frac{n_0}{m} \hbar \vec{\nabla} \varphi(r, t) \quad (6b)$$

The equations of motion and the dispersion relation of the plasma-modes in the superconducting state are also given by Eqs. 3 and 5, with the dissipation $1/\tau$ set to zero, but v_s and ω_p may differ from those in normal state.

IV. STRONG ANISOTROPY

Let us consider now the case of quasi-two dimensional materials, characterized by a large mass along perpendicular to the planes and a light mass along it. For this

case we obtain from Eq. 4 the dispersion relation

$$\omega(\vec{k})^2 = \frac{\omega_{p,p}^2 k_p^2 + \omega_{p,s}^2 k_s^2}{k_p^2 + k_z^2} + v_{s,p}^2 k_p^2 + v_{s,p}^2 k_z^2 \quad (7)$$

Inspection of this expression reveals, that $k = 0$ corresponds to a singular point: If we approach it along the planes, we obtain $\omega(k_p \rightarrow 0, k_z = 0) = \omega_{p,p}$, while along the z-direction $\omega(k_p = 0, k_z \rightarrow 0) = \omega_{p,z}$. In the extreme situation where the material is insulating along the z-direction, one obtains

$$\omega(\vec{k})^2 = \omega_{p,p}^2 \frac{k_p^2}{k_p^2 + k_z^2} + v_{s,p}^2 k_p^2 \quad (8)$$

which corresponds to the small k_z limit of the layered electron gas model^{33,34,35}. In this case $\omega(k_p = 0, k_z \neq 0) = 0$. Moreover, if we consider the dispersion along the plane, while keeping k_z fixed at a finite value, it becomes sound-like: $\omega = v_{eff} k_x$, with a sound velocity $v_{eff}^2 = \omega_{p,p}^2/k_z^2 + v_{s,p}^2$. This behaviour can be measured with k -dependent electron energy loss spectroscopy³⁶.

V. DIELECTRIC FUNCTION

It is straightforward to solve Eq. 3 in the presence of a longitudinal external field $\vec{E}(r, t) = -\vec{\nabla}\phi(r, t)$: The total electric field is the sum of the externally applied field and the field arising from the charge distribution of the matter-field, $\vec{\nabla} \cdot \vec{E}(r, t) = \vec{\nabla} \cdot \vec{E}^e(r, t) + 4\pi e^* n(r, t)$. The longitudinal inverse dielectric function, describing the response to an external charge, is defined as the external field divided by the total field: $\epsilon = \vec{\nabla} \cdot \vec{E}^e / \vec{\nabla} \cdot \vec{E}$. With the help of Eq. 3 the inverse dielectric function is now easily obtained

$$\begin{aligned} \frac{1}{\epsilon(\omega, k)} &= 1 + \frac{4\pi e^* n(r, t)}{\vec{\nabla} \cdot \vec{E}^e(r, t)} \\ &= 1 - \frac{\omega_p^2}{\omega_p^2 + v_s^2 k^2 - \omega(\omega + i/\tau)} \end{aligned} \quad (9)$$

The plasma-modes correspond to the condition that an arbitrarily weak density fluctuation with wave-vector k and frequency ω can generate a finite electromagnetic response \vec{E} . Because $1/\epsilon(\omega, k)$ describes the response to the density fluctuation, in an isotropic fluid these modes have the electrical polarization parallel to the propagation direction. The charge-density modes therefore correspond to the poles of Eq. 9

$$\omega = \frac{1}{2i\tau} \pm \sqrt{\omega_p^2 + v_s^2 k^2 - \frac{1}{4\tau^2}} \quad (10)$$

The relevant limit for optical spectroscopy is $k \rightarrow 0$ for which the mode frequencies become purely imaginary if $1/\tau > 2\omega_p$. This corresponds to the limit of overdamping. This situation is characterized by the fact that

$\text{Re}\epsilon(\omega, k) > 3/4$ for all (real) frequencies. On the other hand, the condensate of a superconductor is characterized by the absence of dissipation, at least for frequencies much smaller than the superconducting gap, implying that $\epsilon(\omega, k) = 0$ *must* occur at some finite frequency. Hence in materials where the dissipation in the normal state is large enough to cause an over-damped charge response, the charge-density collective mode *must* emerge at some finite frequency within the frequency window of dissipation-less flow when the material becomes superconducting at low temperatures.

This kind of behaviour is indeed observed for the c-axis optical response of the cuprate superconductors^{37,38,39,40,41,42,43}. An example of this is shown in Fig. 4. T_c of this crystal was 33 K. At this temperature $\epsilon'(\omega)$ never crosses zero except for the phonons between 200 and 400 cm^{-1} . Below T_c a dissipation-less low-frequency electronic mode appears, characterized by a zero-crossing of $\epsilon'(\omega)$ reaching about 50 cm^{-1} for $T \ll T_c$. Note, that although superconductivity implies the presence of a plasma-mode, the reverse is not true: In fact in most superconductors known to date, the plasmon is *not* overdamped in the normal state, and the transition into the superconducting state affects the plasma-frequency only marginally.

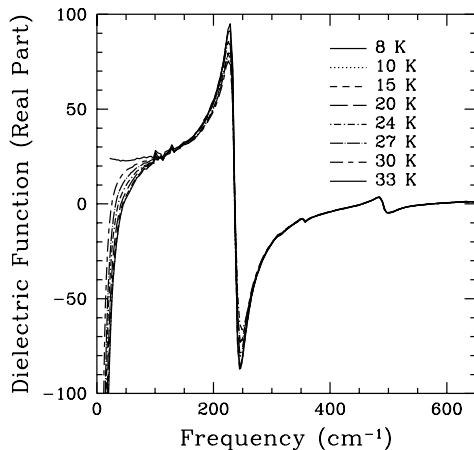


FIG. 4: Dielectric function with polarization along the c-direction of $\text{La}_{1.86}\text{Sr}_{0.14}\text{CuO}_{4+\delta}$ for different temperatures. T_c of this sample is 33 K. The data are from Ref. 44.

A second type of collective mode has the electric field perpendicular to the direction of propagation. Those modes correspond to absorption peaks of the optical conductivity function, $\sigma(\omega) = j/E$, which in the long wavelength limit is proportional to the dielectric function $\sigma_1(\omega) = \omega \text{Im}\epsilon(\omega)/(4\pi)$. In the limit that $k \rightarrow 0$ this condition requires, that an arbitrarily weak electric field results in a finite current. Hence at the transverse collective mode frequency $\sigma(\omega) \rightarrow \infty$. For a single component plasma this happens at $\omega = -i/\tau$. In a super-

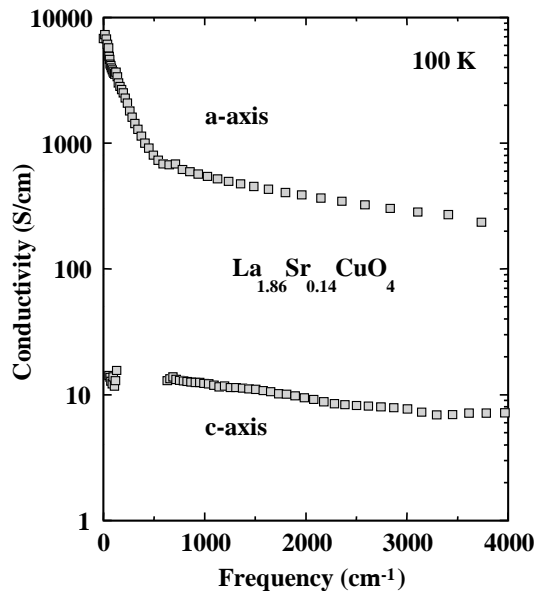


FIG. 5: Optical conductivity with polarization along the planes and along the c-direction of $\text{La}_{1.86}\text{Sr}_{0.14}\text{CuO}_{4+\delta}$ for $T=100$ K. To obtain a high accuracy for the optical conductivity along the c-direction, the transmission coefficient was measured of a 20 μm thick slab, which had been cut along ac-plane. Due to a strong absorption by the optical phonons between 200 and 600 cm^{-1} , no transmission could be detected in this range. Therefore the c-axis optical conductivity is not shown in this range. The data are from Ref. 45.

conductor $1/\tau = 0$, and the condensate causes indeed a diverging conductivity at zero frequency. In a normal metal τ is finite, and the optical conductivity is characterized by a narrow Drude peak. In the cuprates, if the electric field is polarized along the c-direction, a narrow Drude peak is however *not* observed in the frequency dependence of $\sigma(\omega, T)$. Also the temperature dependence of the c-axis conductivity is reminiscent of a semiconductor, at least in samples which are not strongly overdoped. Hence the cuprates have a strong anisotropy between ab-plane and c-axis conductivity in several respects: (i) The DC-resistivity, (ii) the superfluid spectral weight of the superconducting state, (iii) the temperature dependence of the conductivity (iv) and the frequency dependence of the conductivity. Although (i) and (ii) can be easily explained from a large effective mass anisotropy, (iii) and (iv) imply that the transport mechanism itself is anisotropic. These observations, which belong to the oldest and most firmly established features of the cuprate superconductors, have been -and still are- the subject of many speculations, none of which have been completely satisfactory in every respect. Fig. 5 demonstrates an example of this. The strong optical phonons obscure part of the electronic response along the c-axis, but it is clear from this graph that the electronic response has only a weak frequency dependence, and does not appear to agree with the Drude line-shape.

VI. THE MASS OF A PHOTON IN A SUPERCONDUCTOR

A. The Anderson-mechanism for photon-mass generation

For long wavelengths the energy momentum dispersion relation of transverse polarized electromagnetic waves propagating inside the superconductor can be calculated from the relation²⁹ $k^2 c^2 = \epsilon(\omega) \omega^2$ between the wave-vector, the frequency and the dielectric function. In Fig. 1 the data of Fig. 4 have been displayed in this way. This is an example of the Anderson-mechanism discussed in the introduction, which generates a finite mass of the photons by coupling them to a spontaneous symmetry-breaking field. We can see from Fig. 4, that compared to the W- and Z-boson in elementary particle physics this is merely a feather: the photon-gap is about 6 meV, which is 10^{13} times smaller than the mass of the W-boson (80 GeV). The estimated mass of the Higgs-boson⁴⁶ is 10^{13} times larger than the superconducting gap, $\sim 2k_B T_c = 5.5$ meV.

Using a cavity resonance technique operating at a single photon energy, and using a magnetic field to tune the plasma-frequency of the superconductor inside the cavity, the presence of the mass-gap has been demonstrated both for $k \parallel E \parallel c$ and for $k \perp E \parallel c$ in Bi2212^{47,48}.

B. The Tinkham-Ferrell sumrule

A useful and important property of the c-axis optical conductivity concerns the spectral weight sum-rule, or f-sum rule: (i) The spectral weight represented by the zero-frequency δ -function in the superconducting state is represented as the square of the plasma-frequency of the condensate, $\omega_{p,s}^2$. (ii) A consequence of BCS theory is, that the spectral weight at finite frequencies is reduced due to the opening of a gap in the optical conductivity. (iii) The Tinkham-Ferrell sumrule^{49,50,51,52} illustrated in Fig. 6, asserts that the spectral weight of the condensate balances exactly the decrease of optical spectral weight integrated over all frequencies larger than zero, compared to the normal state:

$$\rho_s = \int_{0+}^{\infty} \text{Re}(\sigma_n(\omega, \vec{q}) - \sigma_s(\omega, \vec{q})) d\omega \quad (11)$$

where the wave-vector \vec{q} is introduced in a general framework for the analysis, where all space and time-dependent quantities inside the material are Fourier-analyzed. The above stated sumrule has a general validity, irrespective of the microscopic details, due to the fact that it follows from a strict conservation law (*i.e.* particle number conservation). In recent years the sumrule has been an important instrument to address ideas that superconductivity may be stabilized by interlayer tunneling, or, more generally, to study the direction of change of kinetic energy

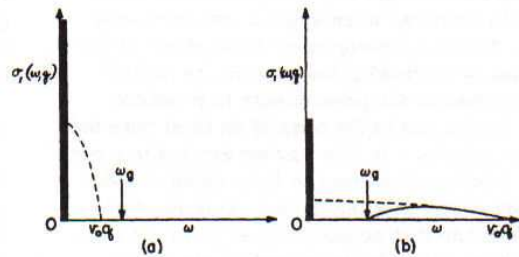


FIG. 6: Figure copied from Ref. 49 by Tinkham and Ferrell. Original caption: "Effect of the superconducting transition on the frequency-dependent conductivity for (a) long- and (b) short-wavelength transverse electromagnetic waves. The normal-state conductivity is indicated by dashed curves and extends to the maximum frequency of $v_0 q$, where v_0 is the Fermi velocity and q is the wave number. In (a) the wavelength is sufficiently long that the maximum absorption frequency in the normal state falls short of the energy gap threshold $\hbar\omega_g$. Consequently essentially all of the oscillator strength is absorbed by the delta function at zero frequency, leading to a full London current. In (b) the shorter wavelength causes the absorptions in the normal state to be spread over a frequency interval much larger than the energy gap. The strength of the delta function is therefore less and the London current is weakened. This dependence of the London current on wavelength is equivalent to the nonlocal current-field relation of Pippard."

when the material becomes superconducting both along the c-direction^{53,54,55,56,57,58,59,60,61,62,63,64,65,66,67,68}, and along the planar direction^{69,70,71,72,73}.

In a BCS superconductor one expects that by and large most of the spectral weight should be recovered on an energy range of 4 times the gap⁷⁴. Experiments with light polarized along the c-axis of the cuprates have revealed that in the underdoped samples a large fraction of the spectral weight remains unrecovered up to 20 times the gap energy^{63,65,75}. At optimal doping the absolute value of non-recovered c-axis spectral weight is even larger (see Fig. 7), but the ratio $\Delta N(\omega_m)/\rho_s \equiv \rho_s^{-1} \int_{0+}^{\omega_m} \text{Re}(\sigma_n(\omega) - \sigma_s(\omega)) d\omega$ decreases due to the fact that ρ_s increases sharply as the doping is increased. Interestingly, in addition to the opening of the superconducting gap, we observed an *increase* of conductivity above the gap up to 270 meV with a maximal effect at about 120 meV⁷⁵. This may indicate a new collective mode at a surprisingly large energy scale²⁵. For the *ab*-direction of underdoped and optimally doped Bi2212 about 0.25% of the *ab*-plane spectral weight remains unrecovered up to about 20 times the gap energy⁷¹. However, in absolute numbers the unrecovered spectral weight is orders of magnitude larger along the planes than along the c-direction.

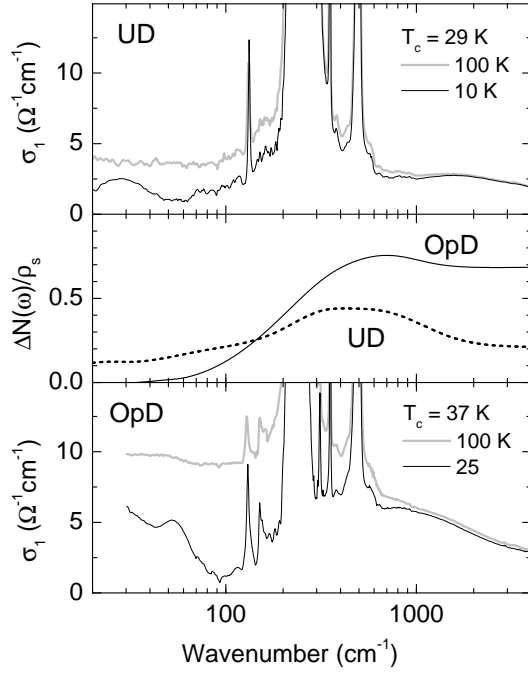


FIG. 7: Optical conductivity of underdoped (top panel) and optimally doped LSCO (bottom panel). In the middle panel the sum-rule check is displayed. The quantity displayed here corresponds to $(N^n(\omega, T) - N^{sc}(\omega, T))/\rho_s(T)$, where the temperature dependent optical conductivity of the normal state has been extrapolated to obtain $N^n(\omega, T)$ and $N^{sc}(\omega, T)$ both at the same temperature below T_c . The details of this analysis are given in Ref. 75.

C. Relation between photon-mass and spectral-weight

The presence of the superconducting condensate contributes a term $-8\rho_s/\omega^2$ to the dielectric function. Because this term diverges for $\omega \rightarrow 0$, and $\epsilon(\omega)$ should become positive for $\omega \rightarrow \infty$, this means that in the superconducting state the dielectric function *must* cross through zero for some finite frequency. This is the plasma-frequency of the superconducting condensate. If the remaining contributions to the dielectric function, ϵ_b , (for example those coming from optical phonons) have a weak frequency dependence in the region where this zero crossing occurs, the plasma frequency of the condensate will be $\omega_{p,s} = (8\rho_s/\epsilon_b)^{1/2}$. In section VIA we have seen that, due to Anderson's mechanism for mass generation, inside a superconductor the photons acquire a gap $\hbar\omega_{p,s}$. For the conditions described above the photon dispersion relation is $\omega^2 = (k^2c^2 + 8\rho_s)/\epsilon_b$. Because the dynamical mass of the photons is $m_A = \hbar/(d^2\omega/dk^2)$, we conclude that the following relation exists between the spectral weight removed from the optical conductivity implied by the Tinkham-Ferrell rule, and the photon-mass inside the

superconductor discussed in the previous section:

$$\rho_s = \frac{m_A^2 c^4}{8\hbar^2 \epsilon_b} \quad (12)$$

In the example given in Fig. 1 we have $\rho_s \simeq 2.5 \cdot 10^{26} \text{ s}^{-1}$, and $\epsilon_b \simeq 22.7$. Using the expressions above, the dynamical mass of c-polarized photons in this compound is then $2.5 \cdot 10^{-34} \text{ g}$, which is about four-million times less than the mass of an electron.

VII. MULTI-COMPONENT PLASMA

The problem of a coupled two-component superconducting plasma has been studied by Leggett. In this model one considers a homogeneous mixture of two liquids, representing two different bands of charge carriers (*e.g.* an s-band and a d-band). Electrons can flow from one band to the other, which introduces a current between the two bands, $\frac{d}{dt}(n_s - n_d)$. The coupling, indicated in Fig. 8b, involves the scattering of a pair of electrons from the s-band to the d-band and *vice versa*. This is a particular (pairing) term in the potential energy. Only if in addition the wave-functions differ on an atomic scale, the flow of charge from one band to the other involves a real motion of electrons. In the somewhat analogous case of longitudinal NMR in 3-He-A, the "bands" are the up- and down-spin states, so it is clear that in that case there is no flow in real space. This contributes a portion to the energy proportional to $(\frac{d}{dt}(n_s - n_d))^2$. The corresponding Hamiltonian is

$$\mathcal{H} = \frac{\kappa n_0^2 \Gamma^2}{4} (\nu_s(r, t) - \nu_d(r, t))^2 + \frac{1}{2\kappa n_0^2} (n_s(r, t)^2 + n_d(r, t)^2) \quad (13)$$

where Γ is a parameter which characterizes the coupling. The second term of the Hamiltonian is equivalent to the term in Eq. 1 describing the compressive strain energy of the two fluids, and can be decomposed into a relative- and a total density fluctuation, $2n_s^2 + 2n_d^2 = (n_s - n_d)^2 + (n_s + n_d)^2$, where only the former has a corresponding coupling term in the Hamiltonian. With these definitions the Hamiltonian equations of motion are

$$\frac{d}{dt}(n_s - n_d) = \kappa n_0^2 \Gamma^2 (\nu_s - \nu_d) \quad (14a)$$

$$\frac{d}{dt}(\nu_s - \nu_d) = -\frac{1}{\kappa n_0^2} (n_s - n_d) \quad (14b)$$

The solution has the form $\delta n(t) = \delta n(0)e^{i\Gamma t}$: This is a collective mode with a frequency Γ , where charge oscillates between the two reservoirs.

Already in a normal metal with two partly occupied bands, excitations exist which correspond to the oscillation of charge between the two bands: From the single electron band structure the lowest optical energy

electron-hole transition occurs at an energy corresponding to the smallest vertical distance between the two bands, for k -values where there is one band above and one below the Fermi energy. This splitting is usually of the order of the bandwidth, *i.e.* of the order of 1 eV, although in principle it can be zero provided that the two bands accidentally cross at E_F (this happens in some of the bucky-tubes).

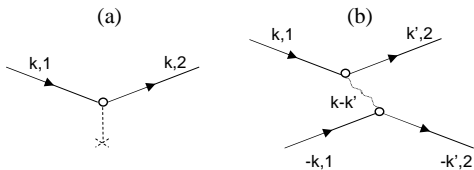


FIG. 8: (a) Interband coupling whereby a single electron is transferred from band 1 to band 2, while conserving momentum. (b) Interband coupling process whereby a pair of electrons is transferred from band 1 to band 2.

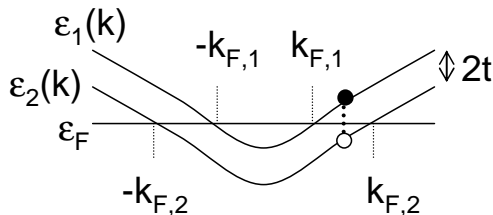


FIG. 9: A doubly degenerate band is split due to an inter-band coupling term t . Electromagnetic radiation at a frequency $2t/\hbar$ can excite the electrons across the split band.

A special case occurs if the two bands are degenerate for all k -values: The presence of an interband-coupling, t scatters electrons between two different bands, while conserving their momentum, k . The eigenstates become symmetric and anti-symmetric combinations of the two original bands at every k -point, split by an energy difference $2t$ (see Figs. 8a and 9). In the optical spectra this splitting causes an absorption band, corresponding to the 'vertical' ($\delta k = 0$) excitations from the occupied 'symmetric' to the unoccupied anti-symmetric band, as indicated in Fig. 9. This absorption is peaked at a frequency $2t/\hbar$, which indicates that in this case Γ represents the single particle inter-band coupling: $\hbar\Gamma = 2t$.

However, the energy of interband-excitations is usually large compared to the superconducting gap. The collective modes discussed by Leggett¹⁶ are of a fundamentally different nature: If the two liquids are superfluids, an additional type of tunneling becomes important, *i.e.* the simultaneous tunneling of a *pair* of electrons. The tunneling-rate of a pair is usually much smaller than that of a single electron, and the collective modes which correspond to the dynamical oscillations of pairs between

the two bands have a correspondingly low energy. If the energy is below the gap for pair-excitations, the dissipation is suppressed, hence these modes can exist by virtue of their low energy. The coupling between the reservoirs, indicated in Fig. 8b, in this case involves the scattering of a *pair* of electrons in band 1 with momentum $(k, -k)$ to a pair in band 2 with momentum $(k', -k')$ due to the interaction between the electrons. In Fig. 8 this interaction is represented by the exchange of a single boson, but more complicated processes may be involved. For coupled superconducting bands $\hbar^{-1}(\nu_s - \nu_d) = \varphi_s - \varphi_d$ is just the phase difference between the two reservoirs¹⁶. In this case the pre-factor of the kinetic energy in Eq. 13, $\kappa n_0 \hbar^2 \Gamma^2$, is nothing but the Josephson coupling between the two reservoirs. If the material is *not* a superconductor, *a priori* there is no reason for the exciton to be absent. However, the gap in the superconducting state removes the dissipation for frequencies below the gap, making multi-band superconductors the best candidates to observe this type of collective mode. At present this type of relative-phase excitons have been reported in two type of superconductors: (i) the high T_c cuprates^{10,76}, and (ii) MgB_2 ^{77,78,79}. In the following section we will discuss the former case in detail.

VIII. LAYERED MATERIALS

The cuprates present a rather special case where the interband Coulomb interactions, which were left out of consideration in the formalism sketched in the previous section, are actually more important than the compressibility term. Following the Lawrence-Doniach model⁸⁰, we consider each plane as an individual charge reservoir, or band. Because we will be mainly interested in collective modes involving currents perpendicular to the planes, we will only deal with the discrete nature of the lattice in the c -direction. As a result it is convenient to define the Hamiltonian and the equations of motion in terms of discrete momentum- ν_j and density-fields n_j (where j is a layer-index) introduced in the previous section, instead of the continuous fields $\nu(r, t)$ and $n(r, t)$, used in section II. The Hamiltonian therefore becomes similar to Eq. 13, but we also want to include a Coulomb interaction between the layer-charges. We already encountered the Coulomb interaction in section II. Because we want to discuss only propagation perpendicular to the planes, we work in the limit of zero charge fluctuations parallel to the planes. Integrating over the planes the Coulomb term of Eq. 1 becomes equivalent to the interaction between parallel plates of charge. The Coulomb energy of two positively charged parallel plates decreases linearly as a function of distance. The Hamiltonian density relevant to the case of c -axis plasmons in layered superconductors

is then¹⁷

$$\mathcal{H} = \frac{\kappa n_0^2}{4} \sum_j \Gamma_{j,j+1}^2 (\nu_j - \nu_{j+1})^2 + \frac{1}{2\kappa n_0^2} \sum_j n_j^2 - \frac{2\pi e^{*2}}{\epsilon_\infty} \sum_{j>l} d_{j,l} n_j n_l \quad (15)$$

where $d_{j,l}$ is the distance between the layers with indices j and l . The other parameters have already been discussed in the previous sections. In Ref. 17,18 the discussion has been limited to the Josephson coupling. In a superconductor $\hbar^{-1}(\nu_j - \nu_{j+1})$ corresponds to the phase difference $\varphi_j - \varphi_{j+1}$ between neighboring layers. However, superconductivity and long-range phase coherence are not a pre-requisite for the validity of Eq.15: Under special conditions the first term of the Hamiltonian corresponds to a Josephson coupling, but more generally it represents the kinetic energy related to the charge flow. It has a finite value due to the fact that the inertial mass of the charge carriers is finite.

IX. PLASMA DISPERSION IN A SINGLE LAYER MATERIAL

We will first discuss the case of a stack of 2D superconducting planes, with lattice constant d along the c -direction, an compressibility κ , and an interlayer coupling Γ . For later use we define here also the Josephson plasma frequency, and a dimensionless constant proportional to the incompressibility

$$\gamma \equiv \frac{\epsilon_\infty}{4\kappa n_0^2 d e^{*2}} \quad (16)$$

$$\omega_J^2 \equiv \frac{2\kappa n_0^2 d e^{*2} \Gamma^2}{\epsilon_\infty} = \frac{1}{2\gamma} \Gamma^2 \quad (17)$$

The Hamiltonian equations of motion, $\frac{dn_j(t)}{dt} = \frac{\partial \mathcal{H}}{\partial \nu_j}$, $\frac{d\nu_j(t)}{dt} = -\frac{\partial \mathcal{H}}{\partial n_j}$, give

$$\begin{aligned} \frac{d^2}{dt^2} n_j &= \frac{\kappa n_0^2 \Gamma^2}{2} \frac{d}{dt} ((\nu_j - \nu_{j+1}) + (\nu_j - \nu_{j-1})) \\ &= \Gamma^2 \frac{n_{j+1} + n_{j-1} - 2n_j}{2} \\ &+ \omega_J^2 \sum_m \frac{2d_{j,m} - d_{j+1,m} - d_{j-1,m}}{2} n_m \end{aligned} \quad (18)$$

The distances between the l th and the j th plane is $d_{j,m} = d|j - m|$. Because $2|j - m| - |j + 1 - m| - |j - 1 - m| = -2\delta_{j,m}$ the only remaining term in the summation over m corresponds to $m = j$. Substituting the plane wave expression, $n_k = \sum_j e^{ikdj} n_j$, in Eq. 18 we obtain the frequency-momentum dispersion relation for Josephson plasmons travelling perpendicular to the planes

$$\omega(k) = \sqrt{\omega_J^2 + 4\gamma \cos^2(kd/2)} \quad (19)$$

For $k = 0$ we obtain the usual value for the Josephson plasma frequency. In addition there is an upward dispersion, which is determined now by the incompressibility parameter γ , similar to the dispersion in the continuum model, Eq. 5.

X. FIELD EFFECT DOPING OF A SINGLE LAYER MATERIAL

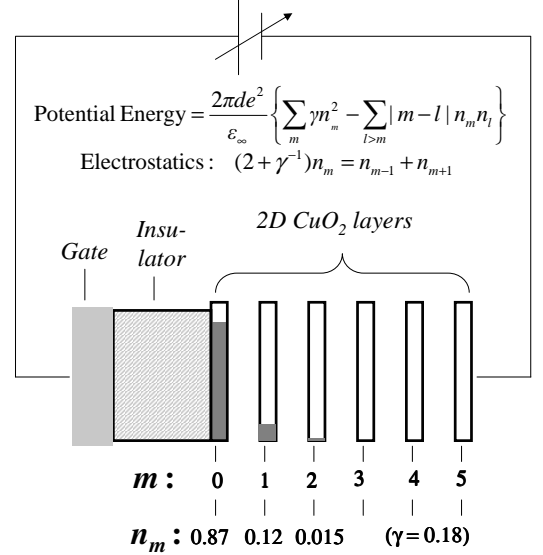


FIG. 10: Doping profile of a field induced layered electron gas.

Some special consideration deserves the doping of insulating parent compounds by the field effect. Field effect devices of high T_c materials are a technological challenge. Although this kind of technology has not yet completely matured, several groups are working into this direction, and a small tuning of the superconducting transition temperature in a cuprate based field effect device has for example already been realized⁸¹.

The doping profile in this layered electron liquid model has a simpler form, than the doping profile in a 3D semiconductor⁸², and the equations are simpler: All we need to do in order to calculate the doping profile below the insulating barrier (see Fig10), is to evaluate Eq. 18 in the static limit. In other words, we have to equate the lefthand side of the expression to zero. Multiplying both sides of the expression with Γ^{-2} we obtain

$$n_{j+1} + n_{j-1} - \left(2 + \frac{1}{\gamma}\right) n_j = 0 \quad (20)$$

which has the following very simple solution

$$\begin{aligned} n_j &= n_0 (1 - f) f^j \\ f &= 1 + \frac{1}{2\gamma} - \frac{1}{2\gamma} \sqrt{1 + 4\gamma} \end{aligned} \quad (21)$$

where $j = 0, 1, 2, \dots$. In section XIII we will see an example of a cuprate for which γ has been measured experimentally, with the result $\gamma = 0.18$. This implies that $f = 0.13$. In other words, in a field effect device for the cuprates (in this example with a lattice spacing of 0.6 nm) the first layer is expected to receive a fraction $1 - f = 0.87$ of the total charge induced by the gate of the field effect device⁸³.

XI. SINGLE BI-LAYER

Let us now consider a single bi-layer, with a bilayer-distance d_K and a coupling frequency $\Gamma_{1,2} \equiv \Gamma_K$ between layers 1 and 2:

$$\begin{aligned} \frac{d^2}{dt^2}(n_1 - n_2) &= \kappa n_0^2 \Gamma_K^2 \frac{d}{dt}(\nu_1 - \nu_2) \\ &= -\kappa n_0^2 \Gamma_K^2 \left(\frac{1}{\kappa n_0^2} + \frac{\pi e^{*2} d_K}{\epsilon_\infty} \right) (\nu_1 - \nu_2) \end{aligned} \quad (22)$$

The first term on the righthand side, Γ_K^2 corresponds to the restoring effect on the non-equilibrium charge density due to the incompressibility term (the second term in Eq.15), whereas the second term, $\omega_K^2 = 2\pi e^{*2} d_K \epsilon_\infty^{-1} \kappa n_0^2 \Gamma_K^2$ is due to the restoring effect of the electric field (the third term in Eq.15). We see, that the resonance frequency of this mode is

$$\Omega_K = \sqrt{\Gamma_K^2 + \omega_K^2} = \Gamma_K \sqrt{1 + \frac{2\pi e^{*2} d_K \kappa n_0^2}{\epsilon_\infty}} \quad (23)$$

The charge and the density appear in the combination $(e^* n_0)^2$, the value of which is independent of whether one defines n_0 and e^* as the density and charge of single electrons, or pairs. In a cuprate superconductor typically $d \sim 6 \cdot 10^{-8}$ cm, $\kappa n_0 \sim 1 \text{eV}^{-1} = 6 \cdot 10^{11} \text{erg}^{-1}$, the electronic density is $n_0 \sim 6 \cdot 10^{14} \text{cm}^{-2}$, and the background dielectric constant $\epsilon_\infty \sim 10$. Without the Coulomb interactions, *i.e.* assuming that $e^* = 0$ in Eq.23, the frequency of the collective mode is Γ_K . However, the elementary charge is $e = 4.8 \cdot 10^{-10} \text{erg}^{1/2} \text{cm}^{1/2}$, and after multiplying all factors we obtain ~ 3 for the second term under the square root. This demonstrates that the 'correction' due to the Coulomb interaction is the dominant contribution to the internal Josephson resonance frequency of the cuprates. In fact in the first publications on this subject only the Coulomb term had been taken into account¹⁸, whereas the second term of Eq. 22 (the term considered by Leggett) was neglected. However, for a correct quantitative description of the optical spectra it is important to take into account all three terms of the hamiltonian Eq. 15.

Let us now consider a crystal composed of a stack of bi-layers of the type described above, where the bi-layers occupy a volume fraction f . For example $f=1/6$ in Bi2212. Let us for the moment ignore the inter-bilayer

hopping. With the model above we obtain for the dielectric function¹⁷

$$\epsilon(\omega) = \epsilon_\infty \frac{\omega^2 - \Omega_K^2}{\omega(\omega + i0^+) - (\Omega_K^2 - f\omega_K^2)} \quad (24)$$

This expression predicts an optical absorption at a frequency $(\Omega_K^2 - f\omega_K^2)^{1/2}$, which is lower than the collective mode of a single bi-layer, Ω_K . This reduction of the transverse polarized collective mode is a consequence of the Coulomb coupling between the bi-layers in the crystal. The longitudinal mode, *i.e.* the frequency for which $\epsilon(\omega) = 0$, is at Ω_K .

XII. STACK OF ALTERNATING STRONG AND WEAK JUNCTIONS

Because it was assumed that there is no coupling between the bi-layers, the screening at low frequencies is not contained in Eq. 24. In order to describe this effect, Eq. 15 needs to be solved with an inter-bilayer coupling taken into account. The result obtained in Refs. 17,84,85,86,87,88 is the following

$$\epsilon(\omega) = \frac{\epsilon_\infty}{\omega^2} \frac{(\omega^2 - \tilde{\omega}_+^2)(\omega^2 - \tilde{\omega}_-^2)}{\omega(\omega + i0^+) - \tilde{\omega}_T^2} \quad (25)$$

where the frequencies $\tilde{\omega}_\pm$ and $\tilde{\omega}_T$ can be expressed in $\Gamma_{K,I}$ (defined in Eq. 15) and $\Omega_{K,I}$ (defined in Eq. 23). We use the indices K and I to indicate the bilayer and the inter-bilayer couplings

$$\begin{aligned} \tilde{\omega}_\pm^2 &= \frac{1}{2} (\Omega_K^2 + \Omega_I^2) \pm \frac{1}{2} \sqrt{(\Omega_K^2 - \Omega_I^2)^2 + 4\Gamma_K^2 \Gamma_I^2} \\ \tilde{\omega}_T^2 &= (1 - f)(\Omega_K^2 + \Gamma_I^2) + f(\Omega_I^2 + \Gamma_K^2) \end{aligned} \quad (26)$$

The notation is slightly different from Ref. 17, allowing more transparent expressions. From this expression we see, that now there are two longitudinal modes (corresponding to $\epsilon(\omega) = 0$) and one transverse mode (a divergence of $\epsilon(\omega)$) at finite frequency. The two extra modes are due to the out-of-phase oscillation of the inter-plane currents in alternating junctions. This situation has been sketched in Fig. 11. In the following sections we will discuss some examples, based on materials where this behaviour has been observed.

XIII. TRANSVERSE OPTICAL PLASMON IN COMPOUNDS WITH WEAK INTERLAYER TUNNELING

The existence of *two* longitudinal modes and *one* associated transverse plasmon mode at finite frequencies has been confirmed experimentally for the $\text{SmLa}_{0.8}\text{Sr}_{0.2}\text{CuO}_{4-\delta}$ in a series of papers^{10,89,90,91,92,93,94,95} (see Figs. 2, and 12). Measurements of the magnetic field and temperature

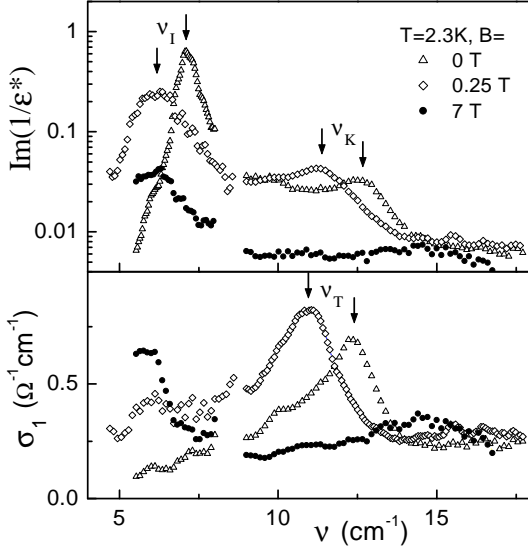
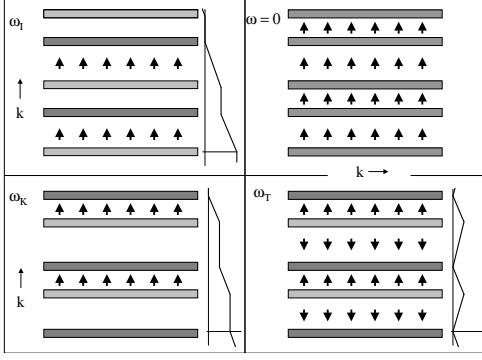


FIG. 12: Real part of the complex conductivity $\sigma_1(\omega)$ and loss function $Im(-1/\epsilon(\omega))$ of $\text{SmLa}_{0.8}\text{Sr}_{0.2}\text{CuO}_{4-\delta}$ along the c -axis for different magnetic fields. The transverse plasmon ν_T is seen as a peak in σ_1 , the longitudinal plasmons $\nu_{I,K}$ as peaks in $Im(-1/\epsilon(\omega))$. The data are from Ref. 93.

dependencies of the longitudinal and transverse plasmons in $\text{SmLa}_{0.8}\text{Sr}_{0.2}\text{CuO}_{4-\delta}$ could be successfully described by the multilayer model explained above, as shown in Fig. 13. It is reassuring, that fits to the data using this model provide for a wide range of temperature and magnetic field the same value for the electronic incompressibility, $\gamma = \epsilon_\infty / (4\pi d e^2 \kappa n_0^2) = 0.18$, where $d = 1.3$ nm is the lattice constant, which is twice the spacing between the layers (see Fig. 14). Note, that the second factor under the denominator of Eq. 23 is just $d_K / (2d\gamma) \simeq 1.4$, close to the estimate given earlier in the discussion. Using the value of $\epsilon_\infty = 23$ in this compound, and $a = 0.38$ nm for the copper-copper distance along the planes, we can use the experimental

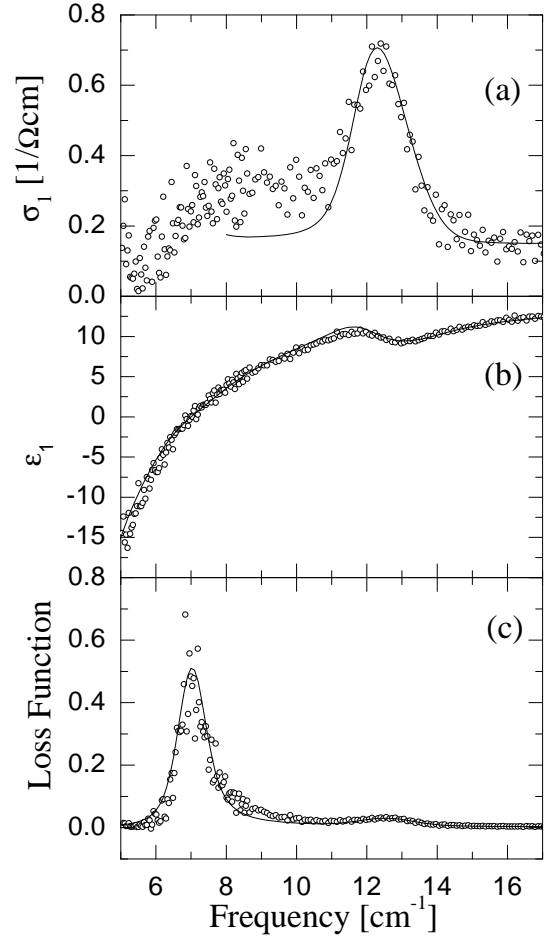


FIG. 13: Fit using Eq. 25, with the parameters defined in Eqs. 26, 23 (solid line) to (a) the real part of the c -axis optical conductivity, (b) Real part of the c -axis dielectric function, (c) the loss function of $\text{SmLa}_{0.8}\text{Sr}_{0.2}\text{CuO}_{4-\delta}$ at 3K. The open circles are the experimental data. The data are from Ref. 10.

value of γ to calculate, that $\kappa n_0^2 a^2 = 0.80$ eV $^{-1}$. In a Fermi liquid picture $\kappa n_0^2 a^2$ is exactly the density of states at E_F per CuO_2 unit, $N(0)$. For the cuprates $N(0) = 0.8$ eV $^{-1}$ is a very reasonable value.

XIV. TRANSVERSE OPTICAL PLASMON AND BI-LAYER SPLITTING IN HIGH T_c CUPRATES

The c -axis optical conductivity $\sigma_1(\omega)$ of YBCO shows several remarkable features^{96,97,98,99,100}: (1) A very low value compared to band structure calculations, reflecting the large ρ_c . (2) A suppression of spectral weight at low frequencies already above T_c in underdoped samples referred to as the opening of a “pseudogap” (which agrees with the upturn in ρ_c). (3) The appearance of an intriguing broad “bump” in the FIR at low T in underdoped samples. The c -axis optical conductivity of YBCO is one order of magnitude larger than for LSCO near optimal doping. As a result the relative importance of the

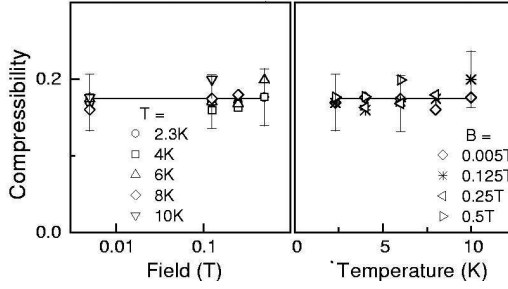


FIG. 14: Upper panels: magnetic field (left) and temperature (right) dependence of the electronic incompressibility, $\gamma = \epsilon_{\infty}/(4\pi de^* \kappa n_0^2)$, of $\text{SmLa}_{0.8}\text{Sr}_{0.2}\text{CuO}_{4-\delta}$. The data are from Ref. 93.

optical phonons in the spectra is diminished. C-axis optical conductivity of underdoped⁹⁶ and optimally and overdoped⁷⁶ YBCO are shown in Fig. 15. Above T_c the optical conductivity is weakly frequency dependent, and does not resemble a Drude peak. Below T_c the conductivity is depleted for frequencies below 500 cm^{-1} , reminiscent of the opening of a large gap, but not an s-wave gap, since a relatively large conductivity remains in this range.

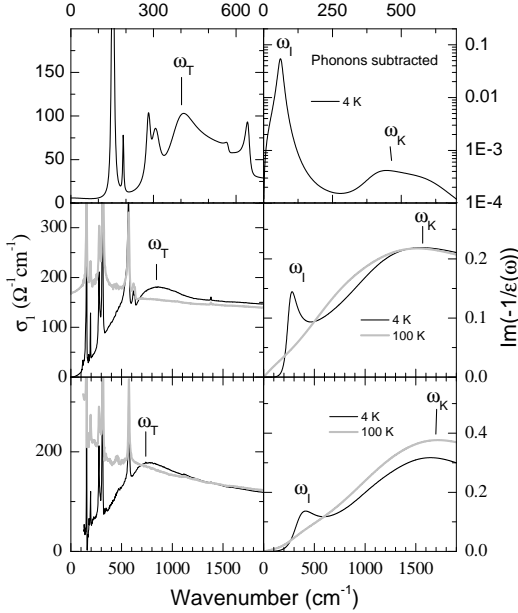


FIG. 15: C-axis optical conductivity (left) and energy loss function (right) as a function of wavenumber (in cm^{-1}) of underdoped ($x=6.6$, top panels), optimally doped ($x=6.93$, middle) and over-doped ($x=7.0$, bottom panel) $\text{YBa}_2\text{Cu}_3\text{O}_{7-x}$. The optical phonons have been subtracted from the loss-functions for clarity. See Refs. 76,96 for details.

There is a slight overshoot of the optical conductivity in the region between 500 and 700 cm^{-1} , and the normal state and superconducting state curves cross at 600 cm^{-1} . Most of the above mentioned issues can be clarified by modelling the cuprates, or in particular

YBCO, as a stack of coupled CuO_2 layers with alternating weaker and stronger links. Indeed, the transverse mode in the infrared spectrum of optimally and overdoped YBCO and the above mentioned “bump” in underdoped YBCO are well fitted by the multilayer model. Hence also the “bump” in the YBCO c-axis spectra may be regarded as a realization of the “excitons” first considered by Leggett¹⁶, which involve the relative phase fluctuations of the condensates formed in two different bands crossing the Fermi surface^{66,67,68,76,101,102,103,104,105}.

This assignment is complicated by the fact, that experimentally the peaks at $\tilde{\omega}_T$ and $\tilde{\omega}_K$ appear at a temperature higher than the superconducting phase transition. For the underdoped samples the intensity of these features has been shown to correlate with the intensity of the spin-flip resonance at (π, π) seen in neutron spectroscopy¹⁰⁶, which is quite far above T_c . On the other hand it appears to be another manifestation of the phenomenon that a strong reduction of dissipation reveals collective modes, which are otherwise overdamped. In the optimally and overdoped cuprate a wide peak is visible in the loss-function around 1600 cm^{-1} for all temperatures. The only effect of the transition into the superconducting state is in this case, that the peak becomes somewhat narrower. This behaviour is reminiscent of a difficulty which we already encountered in the discussion relating to Figs. 8 and 9: The single particle coupling term t between the layers, Fig. 8a, should in principle be revealed in the optical spectrum of the normal state as a transition between the bands consisting of the symmetric and antisymmetric combinations of the two layers^{107,108,109,110,111}. In the underdoped YBCO this process appears to be overdamped. On the other hand, the type of process depicted in Fig. 8b can still contribute at low frequencies, at temperatures where the dissipation becomes sufficiently small. The coherent bi-layer splitting is gradually restored as we move to the optimally and overdoped region. In this case the two types of interlayer transport indicated in Fig. 8 work in parallel, but there is still a temperature dependence, like in the other cases. Note that this does not imply nor require the simultaneous presence of both single electrons and pairs: These are just two different forms of charge transport.

Additional studies of the bi-layer (and tri-layer) materials have provided confirmation of the transverse optical plasmon in these materials. The spectra of the far-infrared c-axis conductivity exhibit dramatic changes of some of the phonon peaks, which correlates with the temperature dependence of the transverse optical plasmon. The most striking of these anomalies can be naturally explained by the local fields acting on the ions arising from the transverse optical plasmon oscillations^{66,67,68,76,101,102,103,104,105,113}.

It is not difficult to extend Eq. 24 for the dielectric function, to cases where the sequence along the c-axis is extended to three or more different junctions per period¹⁸

$$\frac{1}{\epsilon(\omega)} = \sum_m \frac{z_m \omega^2}{\epsilon_\infty (\omega^2 - \omega_{J,m}^2) + 4\pi i \omega \sigma_m} \quad (27)$$

where z_m is the effective volume fraction of the m 'th junction, and σ_m is a parallel dissipative conductivity of the m 'th junction. In tri-layer materials such Bi2223 two of the three junctions are identical because one of the CuO₂-layers is a mirror plane. Consequently the expression above has a degeneracy between two of the three terms in the summation, and the c-axis spectrum should still have one transverse optical plasmon. Interestingly in this case an additional mode exists where the charge oscillations have even parity around the mirror-plane¹¹⁴. This electronic mode is observable with Raman spectroscopy¹¹⁴.

If one introduces a single planar defect layer in an otherwise perfectly periodic stack of Josephson coupled layers, this results in a pronounced satellite line in the real part of the complex resistivity, whose position and amplitude depend on the critical current density and on the parameters of the interlayer coupling¹¹⁵. The extreme narrowness of this plasma-peak could in principle be used to probe the pairing symmetry using a twist grain boundary configuration.

Random variations of the potential barrier, *e.g.* due to chemical disorder, can be taken into account by replacing the summation over m with a weighted integration over $\omega_{J,m}$. If one assumes for example a gaussian distribution, a peak appears in the optical conductivity, which coincides with the center-value of the c-axis plasma frequency¹⁸. This effect is present in all published data of the optical conductivity of LSCO, for example also in Fig. 7. The effect has a strong doping dependence with it's maximum at exactly 1/8 doping¹¹⁶, suggesting an intriguing correlation between disorder in the interlayer Josephson coupling and the tendency toward stripe-formation. This appears to be a manifestation of a more general tendency where disorder allows optical absorption by 'forbidden' collective modes. Similar phenomena have been observed¹¹⁷ along the ab-planes of the cuprates in the THz regime and explained with a model of a planar disordered array of Josephson junctions¹¹⁸.

An alternative way to introduce a more complicated pattern of Josephson couplings along the c-axis is obtained by the application of a magnetic field parallel to the CuO₂ planes, which for YBa₂Cu₃O_{6.6} results in inequivalent insulating layers with and without Josephson

vortices. As a result one optical (transverse) mode appears at around 40 cm⁻¹, corresponding to the antiphase Josephson current oscillations between two inequivalent junctions¹¹⁹.

XV. SUMMARY

In superconductors a rich spectrum of collective modes can be observed using optical techniques. The simplest case is where there is one layer per unit cell, for example La_{2-x}Sr_xCuO₄. Here the Josephson-coupling gives rise to a single c-axis plasmon. This plasmon is an collective mode of the phase of the superconducting order parameter. Their coupling to the electromagnetic field causes a mass-gap of the photons coupled to the superconductor, providing a small energy scale (and small budget) demonstration of the Anderson-Higgs mechanism for generating massive particles. These modes can be described in the context of the Lawrence-Doniach model. However from the optical experiments on SmLa_{0.8}Sr_{0.2}CuO_{4-δ} we have seen that it is important to take into account the fact that the compressibility of the charge-fluid in the layers is finite. The compressibility term establishes the connection to the model considered by Leggett for Josephson coupled bands. A directly observable consequence is the appearance of several additional collective modes in the optical spectrum, which are related to the relative phase excitons predicted by Leggett. However, their energy and optical oscillator strength is strongly affected by the interlayer Coulomb interaction. These excitons have been observed for light polarized along the c-axis in a number of cuprate superconductors. If the number of layers per unit cell is 3 or more, collective modes of even symmetry appear, which can be observed with Raman spectroscopy. In addition to chemical modulation of the interlayer Josephson-coupling, magnetic field parallel to the planes can result in inequivalent insulating layers with and without Josephson vortices.

Acknowledgments

This work was supported by the Swiss National Science Foundation through the National Center of Competence in Research Materials with Novel Electronic Properties-MaNEP.

¹ N. N. Bogoliubov, V. V. Tolmachev and D. V. Shirkov, *A New Method in the Theory of Superconductivity*, (Consultants Bureau, Inc., New York, 1959).

² Y. Nambu, Phys. Rev. Lett. **4**, 380 (1960).

³ J. Goldstone, Nuovo Cimento **19**, 154 (1961).

⁴ P. W. Anderson Phys. Rev. **112**, 1900-1916 (1958)

⁵ P. W. Anderson Phys. Rev. **110**, 985-986 (1958)

⁶ P. W. Anderson Phys. Rev. **110**, 827-835 (1958)

⁷ P. W. Anderson Phys. Rev. **130**, 439-442 (1963)

⁸ P. W. Higgs Phys. Rev. Lett. **13**, 509 (1964)

⁹ P. W. Higgs Phys. Rev. Lett. **145**, 1156 (1967)

¹⁰ D. Dulic, A. Pimenov, D. van der Marel, *et al.*, Phys. Rev.

- Lett. **86**, 4144 (2001).
- ¹¹ D. van der Marel, Phys. Rev. B. **51**, 1147 (1995).
 - ¹² A. Bardasis, and J. R. Schrieffer, Phys. Rev. **121** 1050 (1960).
 - ¹³ R. Sooryakumar and M.V. Klein, Phys. Rev. Lett. **45**, 660 (1980).
 - ¹⁵ P.B. Littlewood and C. M. Varma, Phys. Rev. Lett. **47**, 811 (1981).
 - ¹⁵ C. M. Varma, cond-mat/0109409 (2001).
 - ¹⁶ A. J. Leggett, Prog. Theor. Phys. **36**, 901 (1966).
 - ¹⁷ D. van der Marel, and A. A. Tsvetkov, Phys. Rev. B **64**, 024530 (2001).
 - ¹⁸ D. van der Marel D, and A. Tsvetkov, Czech J. Phys. **46**, 3165 (1996).
 - ¹⁹ D. M. Ginsberg, P. L. Richards, and M. Tinkham, Phys. Rev. Lett. **3**, 337 (1959).
 - ²⁰ V. G. Vaks, V. M. Galitskii, and A. I. Larkin, Sov. Phys. JETP **14**, 1177 (1962).
 - ²¹ Bourges P, Keimer B, Regnault LP, *et al.*, J. Suprcond. **13**, 735 (2000).
 - ²² P. Bourges, Y. Sidis, H.F. Fong, *et al.*, Science **288**, 1234 (2000).
 - ²³ E. Demler, S.-C. Zhang, N. Bulut, and D. J. Scalapino, Int. J. Mod. Phys. B **10**, 2137 (1996).
 - ²⁴ E. Demler, S.-C. Zhang, Phys. Rev. Lett. **75**, 4126 (1995).
 - ²⁵ P. A. Lee, N. Nagaosa, Phys. Rev. B **68**, 024516 (2003).
 - ²⁵ V. G. Vaks, V. M. Galitskii, and A. I. Larkin, Sov. Phys. JETP **14**, 1177 (1962).
 - ²⁶ H.F. Fong *et al.*, Phys. Rev. Lett. **75**, 316 (1995).
 - ²⁷ D. Vollhardt, and P. Wolfe, The superfluid phases of Helium 3, Edited by Taylor and Francis (1990).
 - ²⁸ Herbert Goldstein, Classical Mechanics, Addison-Wesley, Reading, MA, 1980
 - ²⁹ The wave-equation for the transverse modes are $\frac{d^2}{dt^2}\vec{\eta}(r) = \vec{\nabla} \times \frac{n_0}{m} \cdot (e^* \vec{E}(r) - \vec{\nabla} \int d^3r' \frac{e^{*2}n(r')}{|r-r'|} - \frac{\vec{\nabla}n(r)}{\kappa n_0^2} - \frac{\vec{\nabla}\nu(r)}{\tau})$. For waves travelling along one of the principle axis of the mass tensor: $\frac{d^2}{dt^2}\vec{\eta}(r) = -\frac{e^*n_0}{m} \frac{d}{dt}\vec{B}(r,t)$. Solving this together with the Maxwell equations yields the polariton dispersion relation $k^2c^2 = \omega^2\epsilon(\omega)$.
 - ³⁰ G. D. Mahan, Many-Particle Physics, 2d Edition Plenum 1990.
 - ³¹ K. S. Singwi, M. P. Tosi, R. H. Land, and A. Sjölander, Phys. Rev. **176**, 589 (1968).
 - ³² A. vom Felde, J. Sprösser-Prou, and J. Fink, Phys. Rev. B **40**, 10181 (1968).
 - ³³ V.Z. Kresin, and H. Morawitz, Phys. Rev. B **37**, 7854 (1988).
 - ³⁴ S. M. Bose, and P. Longe, J. Phys. Condens Matter **4**, 1799 (1992).
 - ³⁵ A. L. Fetter, Ann. Phys. **88**, 1 (1974).
 - ³⁶ K. Schulte, M.A. James, P.G. Steeneken, G. A. Sawatzky, R. Suryanarayanan, G. Dhalenne, A. Revcolevschi, cond-mat/0010475
 - ³⁷ M. Tachiki, T. Koyama, and S. Takahashi, Phys. Rev. B **50**, 7065 (1994).
 - ³⁸ H. A. Fertig and S. Das Sarma, Phys. Rev. Lett. **65**, 1482 (1990).
 - ³⁹ Hwang EH, Dassarma S, Phys. Rev. B **52**, R7010 (1995).
 - ⁴⁰ L. N. Bulaevskii, M. P. Maley, and M. Tachiki, Phys. Rev. Lett. **74**, 801 (1995).
 - ⁴¹ K. Tamasaku, Y. Nakamura, and S. Uchida, Phys. Rev. Lett. **69**, 1455 (1992).
 - ⁴² O. K. C. Tsui, N. P. Ong, Y. Matsuda, Y. F. Yan, and J. B. Peterson, Phys. Rev. Lett. **73**, 724 (1994).
 - ⁴³ Y. Matsuda, M. B. Gaifullin, K. Kumagai, K. Kadowaki, and T. Mochiku, Phys. Rev. Lett. **75**, 4512 (1995).
 - ⁴⁴ Kim JH, Somal HS, Czyzyk MT, *et al.*, Physica C **247**, 297 (1995).
 - ⁴⁵ D. van der Marel, A. Tsvetkov, M. Grueninger, D. Dulic, H.J.A. Molegraaf, Physica C **341-348**, 1531 (2000).
 - ⁴⁶ Maria Krawczyk, Acta Phys. Polon. B **29**, 3543 (1998)
 - ⁴⁷ K. Kadowaki, I. Kakeya, M. B. Gaifullin, T. Mochiku, S. Takahashi, T. Koyama, M. Tachiki, Phys. Rev. B **56**, 5617 (1997).
 - ⁴⁸ K. Kadowaki, I. Kakeya, and K. Kindo, Europhys. Lett. **42**, 203-208 (1998).
 - ⁴⁹ M. Tinkham and R. A. Ferrell, Phys. Rev. Lett. **2**, 331 (1959).
 - ⁵⁰ R. E. Glover, and M. Tinkham, Phys. Rev. **108**, 243 (1957).
 - ⁵¹ R. E. Glover, and M. Tinkham, Phys. Rev. **110**, 778 (1958).
 - ⁵² P. L. Richards, and M. Tinkham, Phys. Rev. Lett. **1**, 318 (1958).
 - ⁵³ S. Chakravarty, A. Sudbo, P. W. Anderson, and S. Strong, Science **261**, 337 (1993).
 - ⁵⁴ P. W. Anderson, Science **268**, 1154 (1995).
 - ⁵⁵ A. J. Leggett, Science **274**, 587 (1996).
 - ⁵⁶ D. van der Marel, H.S. Somal, B.J. Feenstra, J.E. van der Eb, J. Schuetzmann, Jae Hoon Kim. Proc. 10th Ann. HTS Workshop on Physics, Houston, World Sc. Publ., page 357 (1996).
 - ⁵⁷ J. Schuetzmann, H.S. Somal, A.A. Tsvetkov, D. van der Marel, G. Koops, N. Kolesnikov, Z.F. Ren, J.H. Wang, E. Brueck and A.A. Menovski, Phys. Rev. B **55**, 11118 (1997).
 - ⁵⁸ K. A. Moler, J. R. Kirtley, D. G. Hinks, T. W. Li, and Ming Xu, Science **279**, 1193 (1998).
 - ⁵⁹ A. Tsvetkov, D. van der Marel, K. A. Moler, J. R. Kirtley, J. L. de Boer, A. Meetsma, Z. F. Ren, N. Kolesnikov, D. Dulic, A. Damascelli, M. Grueninger, J. Schützmann, J. W. van der Eb, H. S. Somal, and J. H. Wang, Nature **395**, 360 (1998).
 - ⁶⁰ S. Chakravarty, Eur. Phys. J. B **5**, 337 (1998).
 - ⁶¹ J. R. Kirtley, K.A. Moler, G. Villard, A. Maignan, Phys. Rev. Lett. **81**, 2140 (1998).
 - ⁶² M.B. Gaifullin, Yuji Matsuda, N. Chikumoto, J. Shimoyama, K. Kishio, and R. Yoshizaki, Phys. Rev. Lett. **83**, 3928 (1999).
 - ⁶³ D. N. Basov, S. I. Woods, A. S. Katz, E. J. Singley, R. C. Dynes, M. Xu, D. G. Hinks, C. C. Homes, M. Strongin, Science **283**, 49 (1999).
 - ⁶⁴ S. Chakravarty, H. Kee, E. Abrahams, Phys. Rev. Lett. **82**, 2366 (1999).
 - ⁶⁵ D. N. Basov, C. C. Homes, E. J. Singley, M. Strongin, T. Timusk, G. Blumberg, and D. van der Marel, Phys. Rev. B **63**, 134514 (2001).
 - ⁶⁶ Dominik Munzar, Christian Bernhard, Todd Holden, Andrzej Golnik, Josef Humlicek, and Manuel Cardona, Phys. Rev. B **64**, 024523 (2001).
 - ⁶⁷ Dominik Munzar, Todd Holden, Christian Bernhard, Phys. Rev. B **67**, R020501 (2003).
 - ⁶⁸ A.V Boris, D. Munzar, N.N. Kovaleva, B. Liang, C.T. Lin, A. Dubroka, A.V. Pimenov, T. Holden, B. Keimer, Y. -L. Mathis, C. Bernhard, Phys. Rev. Lett. **89**, 277001 (2002).
 - ⁶⁹ J. E. Hirsch, Physica C **199**, 305 (1992).

- ⁷⁰ J. E. Hirsch, *Physica C* **201**, 347 (1992).
- ⁷¹ H. J. A. Molegraaf, C. Presura, D. van der Marel, P. H. Kes, M. Li, *Science* **295**, 2239 (2002).
- ⁷² A.F. Santander-Syro, R.P.S.M. Lobo, N. Bontemps, Z. Konstantinovic, Z.Z. Li, H. Raffy, *Europhys. Lett.* **62**, 568 (2003)
- ⁷³ D. van der Marel, "Optical signatures of electron correlations in the cuprates." Chapter in "Strong interactions in low dimensions", Edited by D. Baeriswyl and L. Degiorgi, in press, Kluwer (2004); cond-mat/0301506.
- ⁷⁴ However, a not widely realized consequence of BCS theory is, that in fact a small amount of superconductivity induced spectral weight transfer should occur between the Drude peak and the interband transitions, provided that the electrons have a non-parabolic $\epsilon(k)$ dispersion; D. van der Marel, H. J. A. Molegraaf, C. Presura and I. Santos Superconductivity by kinetic energy saving? Chapter in "Concepts in electron correlation", Edited by A. Hewson and V. Zlatić, Kluwer (2003), p 7-16.; cond-mat/0302169.
- ⁷⁵ A. B. Kuzmenko, N. Tombros, H. J. A. Molegraaf, M. Grueninger, D. van der Marel, and S. Uchida, *Phys. Rev. Lett.* **91**, 037004 (2003).
- ⁷⁶ M. Grueninger, D. van der Marel, A.A. Tsvetkov, A. Erb, *Phys. Rev. Lett.* **84**, 1757 (2000).
- ⁷⁷ Agterberg DF, Demler E, Janko B, *Phys. Rev. B* **66**, 214507 (2002).
- ⁷⁸ A. Brinkman, S.H.W. van der Ploeg, A. A. Golubov, H. Rogalla, T. H. Kim, and J. S. Moodera, proceedings of SNS04, Sitges, Spain (2004).
- ⁷⁹ Ya. G. Ponomarev, S. A. Kuzmichev, M. G. Mikheev, M. V. Sudakova, S. N. Tchesnokov, N.Z. Timergaleev, A. V. Yargin, E. G. Maksimov, S. I. Krasnosvobodtsev, A. V. Varlashkin, M. A. Hein, G. Müller, H. Piel, L. G. Sevast'yanova, O. V. Kravchenko, K. P. Burdina, and B. M. Bulychiev, *Solid State Commun.* **129**, 85 (2004).
- ⁸⁰ W. E. Lawrence and S. Doniach in *Proceedings of the 12th International Conference on Low Temperature Physics, Kyoto, 1970*, edited by E. Kanda (Keigaku, Tokyo, 1970).
- ⁸¹ C.H. Ahn, J.M. Triscone and J. Mannhart, *Nature* **424**, 1015 (2003)
- ⁸² Samuel Wehrli, Didier Poilblanc, T. M. Rice, *Eur. Phys. J. B* **23**, 345 (2001)
- ⁸³ The field induced charge is the gate voltage divided by the capacitance of the device, both of which can be measured. Let's suppose for example that the superconducting T_c would be suppressed at a doping level of 1/8 hole per a^2 , i.e. per 2D unit cell. The top layer receives the fraction $1-f$ of the field induced charge, and consequently the suppression of T_c will be delayed to $0.125/(1-f) = 0.156$ field induced holes per a^2 . Hence the quantitative analysis of this delay can be used to obtain an independent measurement of the electronic compressibility in the CuO_2 planes.
- ⁸⁴ Koyama T, *J. Phys. Soc. Jpn.* **71**, 2986 (2002).
- ⁸⁵ Helm C, Bulaevskii LN, *Phys. Rev. B* **66**, 094514 (2002).
- ⁸⁶ Helm C, Bulaevskii LN, Chudnovsky EM, *et al.*, *Phys. Rev. Lett.* **89**, 057003 (2002).
- ⁸⁷ Bulaevskii LN, Helm C, *Phys. Rev. B* **66**, 174505 (2002).
- ⁸⁸ Bulaevskii LN, Helm C, Bishop AR, *et al.*, *Europhys. Lett.* **58**, 415 (2002).
- ⁸⁹ Shibata H, Yamada T, *Phys. Rev. Lett.* **81**, 3519 (1998).
- ⁹⁰ Kakeshita T, Uchida S, Kojima KM, *et al.*, *Phys. Rev. Lett.* **86**, 4140 (2001).
- ⁹¹ Shibata H, *Physica C* **362**, 92 (2001).
- ⁹² Shibata H, *Phys. Rev. Lett.* **86**, 21225 (2001).
- ⁹³ Pimenov A, Loidl A, Dulic D, *et al.*, *Phys. Rev. Lett.* **87**, 177003 (2001).
- ⁹⁴ Shibata H, *Phys. Rev. B* **65**, 180507 (2002).
- ⁹⁵ Shibata H, *Physica C* **367**, 360 (2002).
- ⁹⁶ C.C. Homes, T. Timusk, D.A. Bonn, R. Liang, and W.N. Hardy, *Can. J. Phys.* **73**, 663 (1995).
- ⁹⁷ J. Schützmann *et al.*, *Phys. Rev. B* **52**, 13665 (1995).
- ⁹⁸ S. Tajima *et al.*, *Phys. Rev. B* **55**, 6051 (1997).
- ⁹⁹ R. Hauff *et al.*, *Phys. Rev. Lett.* **77**, 4620 (1996).
- ¹⁰⁰ C. Bernhard *et al.*, *Phys. Rev. Lett.* **80**, 1762 (1998).
- ¹⁰¹ Zelezny V, Tajima S, Motohashi T, *et al.*, *J. Low Temp. Phys.* **117**, 1019 (1999).
- ¹⁰² Munzar D, Bernhard C, Golnik A, *et al.*, *J. Low Temp. Phys.* **117**, 1049 (1999).
- ¹⁰³ Munzar D, Bernhard C, Golnik A, *et al.*, *Solid State Commun.* **112**, 365 (1999).
- ¹⁰⁴ Munzar D, Bernhard C, Golnik A, *et al.*, *Phys. Status Solidi B* **215**, 557 (1999).
- ¹⁰⁵ Bernhard C, Munzar D, Golnik A, *et al.*, *Phys. Rev. B* **61**, 618 (2000).
- ¹⁰⁶ Timusk T, Homes CC, *Solid State Commun.* **126**, 63 (2003).
- ¹⁰⁷ Gartsstein YN, Rice MJ, van der Marel D, *Phys. Rev. B* **49**, 6360 (1994).
- ¹⁰⁸ Forsthofer F, Kind S, Keller J, *Phys. Rev. B* **53**, 14481 (1996).
- ¹⁰⁹ Atkinson WA, Carbotte JP, *Phys. Rev. B* **55**, 3230 (1997).
- ¹¹⁰ Dordevic SV, Singley EJ, Kim JH, *et al.*, *Phys. Rev. B* **69**, 094511 (2004).
- ¹¹¹ Shah N, Millis AJ, *Phys. Rev. B* **65**, 024506 (2002).
- ¹¹² Zelezny V, Tajima S, Munzar D, *et al.*, *Phys. Rev. B* **63**, 060502 (2001).
- ¹¹³ Kovaleva NN, Boris AV, Holden T, *et al.*, *Phys. Rev. B* **69**, 054511 (2004).
- ¹¹⁴ Munzar D, Cardona M, *Phys. Rev. Lett.* **90**, 077001 (2003).
- ¹¹⁵ Gurevich A, Tachiki M, *Phys. Rev. Lett.* **83**, 183 (1999).
- ¹¹⁶ Dordevic SV, Komiya S, Ando Y, *et al.*, *Phys. Rev. Lett.* **91**, 167401 (2003).
- ¹¹⁷ Corson J, Orenstein J, Oh S, *et al.*, *Phys. Rev. Lett.* **85**, 2569 (2000).
- ¹¹⁸ Barabash SV, Stroud D, *Phys. Rev. B* **67**, 144506 (2003).
- ¹¹⁹ Kojima KM, Uchida S, Fudamoto Y, *et al.*, *Phys. Rev. Lett.* **89**, 247001 (2002).